Convergence Acceleration of Iterative Solvers for the Finite Element Analysis Using the Implicit and Explicit Error Correction Methods

AUTHOR(S):

Mifune, Takeshi; Moriguchi, Soichl; Iwashita, Takeshi; Shimasaki, Masaaki

Convergence Acceleration of Iterative Solvers for the Finite Element Analysis Using the Implicit and Explicit Error Correction Methods

Takeshi Mifune[1], Soichi Moriguchi[1], Takeshi Iwashita[2], and Masaaki Shimasaki[3]

[1]Department of Electrical Engineering, Kyoto University, Kyoto 615-8510, Japan
[2]Academic Center for Computing and Media Studies, Kyoto University, Kyoto 606-8501, Japan
[3]Department of Applied Nuclear Engineering, Fukui University of Technology, Fukui 910-8505, Japan

Our previous paper proposed two frameworks for iterative linear solvers: the implicit and explicit error correction methods. In this paper, we discuss the convergence property of these methods. A formula we derive explains the reasonability of the auxiliary matrix that Kameari suggested for thin elements. Additionally, an enhanced auxiliary matrix is devised for thin elements, in which the material property changes discontinuously.

***Index Terms*—Finite element (FE) analysis, iterative solver, preconditioning, thin elements.**

I. Introduction

THE finite element (FE) method is widely used in the numerical analyses of electromagnetic fields. Since the FE formulation generally leads to a large sparse linear system of equations, using an efficient iterative solver is effective in reducing the computation costs of an FE analysis.

Previously, some of the authors proposed two comprehensive frameworks for iterative linear solvers: the implicit error correction (IEC) and explicit error correction (EEC) methods [1], [2]. The singularity decomposition technique (SDT), proposed by Kameari in [3], can be regarded as a special case of the IEC method. A common characteristic of these methods is the use of special auxiliary matrices.

As discussed in [1] and [2], the IEC and EEC methods contain well-known valuable methods, e.g., the $A-\varphi$ method and the multigrid method. Moreover, several numerical examples [1]–[3] have shown that the IEC and EEC methods using appropriate auxiliary matrices accelerate convergence of iterative linear solvers. Nevertheless, from a theoretical viewpoint, little is known about the general relationship between the property of auxiliary matrices and the speed of convergence of iterative solvers.

In this paper, we derive a formula, which gives an estimate of the convergence radius of the IEC method based on a Jacobi iteration. The formula explains the reasonability of the auxiliary matrix, which is proposed in [3] for thin elements.

In addition, we devise a particular auxiliary matrix for sequences of thin elements, in which the material property changes discontinuously. The performance of the IEC and EEC solvers are compared in 2-D and 3-D numerical tests.

II. Implicit and Explicit Error Correction Methods

A. Implicit Error Correction Method

Consider solving the following linear system of equations:

$$A\boldsymbol{x}=\boldsymbol{b}. \tag{1}$$

Here, A, $\boldsymbol{x}$, and $\boldsymbol{b}$ denote an $m\times m$ coefficient matrix, the unknown vector, and the right-hand side vector, respectively.

Manuscript received October 07, 2008. Current version published February 19, 2009. Corresponding author: T. Mifune (e-mail: mifune@fem.kuee.kyoto-u.ac.jp).

Digital Object Identifier 10.1109/TMAG.2009.2012636

The IEC method leads to the following linear equations:

$$\begin{pmatrix} A & AB \\ CA & D \end{pmatrix}\begin{pmatrix} \boldsymbol{y}_1 \\ \boldsymbol{y}_2 \end{pmatrix}=\begin{pmatrix} \boldsymbol{b}_1 \\ \boldsymbol{b}_2 \end{pmatrix}=\begin{pmatrix} \boldsymbol{b} \\ \boldsymbol{b}_2 \end{pmatrix} \tag{2}$$

where B, C, D, and $\boldsymbol{b}_2$ represent auxiliary matrices and the auxiliary vector. The sizes of B, C, and D are $m\times n$, $n\times m$, and $n\times n$, respectively. When a solution is obtained for (2), the solution $\boldsymbol{x}$ in (1) is given by $\boldsymbol{y}_1+B\boldsymbol{y}_2$.

When we choose $C=B^T$, $D=B^TAB$, and $\boldsymbol{b}_2=B^T\boldsymbol{b}$, the IEC formulation (2) corresponds to the SDT [3]

$$\begin{pmatrix} A & AB \\ B^TA & B^TAB \end{pmatrix}\begin{pmatrix} \boldsymbol{y}_1 \\ \boldsymbol{y}_2 \end{pmatrix}=\begin{pmatrix} \boldsymbol{b}_1 \\ \boldsymbol{b}_2 \end{pmatrix}=\begin{pmatrix} \boldsymbol{b} \\ B^T\boldsymbol{b} \end{pmatrix}. \tag{2a}$$

Equations (2) and (2a) can be recognized as generalized forms, which contain the $A-\varphi$ method and the implicit correction multigrid method [1]–[3].

Suppose A is a symmetric positive-definite matrix. Without loss of generality, let the diagonal entries of A and B^TAB be unity. Then, the Jacobi iteration for (2a) gives the approximate solution $\boldsymbol{z}$ for (1), which satisfies

$$\frac{\|(\boldsymbol{x}-\boldsymbol{z}_{\mathrm{new}})\|_A}{\|(\boldsymbol{x}-\boldsymbol{z})\|_A}\le\left\|(I-A-BB^TA)\right\|_A\le\sqrt{2}\max(\alpha+\beta,\gamma). \tag{3}$$

(See Appendix I for the proof.) Here

$$\alpha=\sup_{\boldsymbol{v}\in R(B),\|\boldsymbol{v}\|_A=1}\|A\boldsymbol{v}\|_A \tag{4}$$

$$\beta=\sup_{\boldsymbol{v}\in R(B),\|\boldsymbol{v}\|_A=1}\left\|(I-BB^TA)\boldsymbol{v}\right\|_A=\sup_{\|B\boldsymbol{u}\|_A=1}\left\|B(I-B^TAB)\boldsymbol{u}\right\|_A \tag{5}$$

$$\gamma=\sup_{\boldsymbol{v}\in S(B),\|\boldsymbol{v}\|_A=1}\|(I-A)\boldsymbol{v}\|_A \tag{6}$$

where I, $R(B)$, and $S(B)$ denote the unit matrix, the range of B, and the A-orthogonal complement of $R(B)$, respectively.

Inequality (3) helps us construct B appropriately. Rapid convergence is achieved by setting B so as to decrease α, β, and γ, although this is not a necessary, but sufficient condition.

Note that $I-A$ in (6) is the iteration matrix of the ordinary Jacobi method. In general, the slow convergence components $\boldsymbol{v}$ in iterative methods for (1) have the characteristic that $\|\boldsymbol{v}^TA\boldsymbol{v}\|/\|\boldsymbol{v}^T\boldsymbol{v}\|$ is small. [Although the components for which $\|\boldsymbol{v}^TA\boldsymbol{v}\|/\|\boldsymbol{v}^T\boldsymbol{v}\|$ is large also cause a deterioration in the convergence of the Jacobi method, this is overcome, for example, by conjugate gradient (CG) acceleration.] If we can ensure that

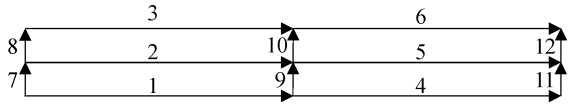

Fig. 1. Thin elements in 2-D edge-element analysis.

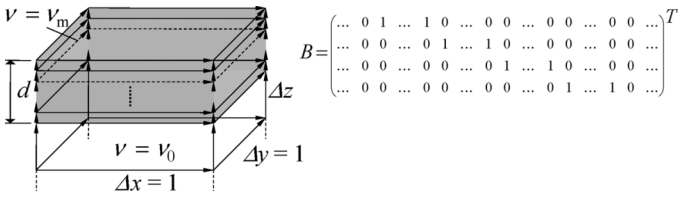

Fig. 2. Thin elements in 3-D edge-element analysis.

$R(B)$ represents approximately the subspace spanned by the slow convergence components, it is expected to decrease α and γ. Stated concisely, this corresponds to the strategy referred to in [3], to ensure that the $\|B_i^T A B_i\|$ are small (before diagonal scaling). Here, B_i is the ith column vector of B.

Meanwhile, we focus additional attention on decreasing β in (5). This is sufficiently achieved by ensuring that $B^T AB$ is approximately equal to the unit matrix (after diagonal scaling).

B. Explicit Error Correction Method

An iterative solver using the EEC method, and which is based on the Gauss–Seidel method, is described below. A single step of the iterative solver can also be used as a precontitioner for a Krylov subspace solver.

i) Update the approximate solution vector $\tilde{\boldsymbol{x}}$ by a Gauss–Seidel sweep for (1).
ii) Execute an EEC procedure [1].
— Compute $\boldsymbol{f} = B^T(\boldsymbol{b} - A\tilde{\boldsymbol{x}})$.
— By applying a Gauss–Seidel sweep to $(B^T AB)\boldsymbol{u} = \boldsymbol{f}$, obtain $\tilde{\boldsymbol{u}}$ that is an approximation of $\boldsymbol{u}$.
— $\tilde{\boldsymbol{x}} \leftarrow \tilde{\boldsymbol{x}} + B\tilde{\boldsymbol{u}}$.
iii) If the iteration does not converge, go to i).

This algorithm can be regarded as an efficient implementation of the Gauss–Seidel iteration for (2a). See Appendix II.

III. Auxiliary Matrix for Thin Elements

Fig. 1 shows an example of thin elements in a 2-D edge-element analysis. The auxiliary matrix B proposed in [3] is constructed by grouping long parallel edges, i.e., $(1, 2, 3)$ and $(4, 5, 6)$

$$B = B_e = \begin{pmatrix} 1 & 1 & 1 & 0 & 0 & 0 & 0 & \dots & 0 \\ 0 & 0 & 0 & 1 & 1 & 1 & 0 & \dots & 0 \end{pmatrix}^T. \quad (7)$$

As mentioned in [3], the above matrix ensures that the $\|B_i^T AB_i\|$ are small. In the 2-D case, furthermore, we can confirm that off-diagonal entries of $B^T AB$ are exactly zero, which leads to $\beta = 0$.

For the 3-D case, Fig. 2 shows a typical example. According to (10), $B^T AB$ is given by

$$\frac{\nu_0}{3\Delta z}\begin{pmatrix} 2 & 1 & 0 & 0 \\ 1 & 2 & 0 & 0 \\ 0 & 0 & 2 & 1 \\ 0 & 0 & 1 & 2 \end{pmatrix} + \frac{\nu_0 \Delta z}{3}\begin{pmatrix} 2 & -2 & -2 & 2 \\ -2 & 2 & 2 & -2 \\ -2 & 2 & 2 & -2 \\ 2 & -2 & -2 & 2 \end{pmatrix}$$

$$+\nu_m d \begin{pmatrix} 2 & -2 & -2 & 2 \\ -2 & 2 & 2 & -2 \\ -2 & 2 & 2 & -2 \\ 2 & -2 & -2 & 2 \end{pmatrix}. \quad (8)$$

Although the matrix above is not a diagonal matrix, the off-diagonal entries are small compared with the diagonal entries, if d and Δz are enough small.

Moreover, for the problem addressed in the next section, we propose an advanced strategy for sequences of thin elements, in which the material property changes discontinuously. A new auxiliary matrix B'_e is constructed by grouping edges, which are included by the same material. An example is shown in Fig. 3. For nodal element analyses, we use a matrix B_n, a simple expansion of (7), as shown in Fig. 4.

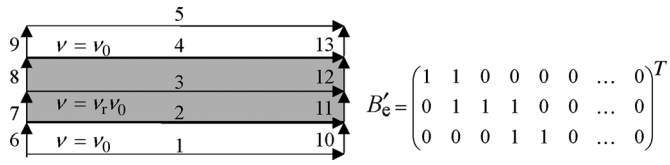

Fig. 3. Thin elements, in which material property changes discontinuously.

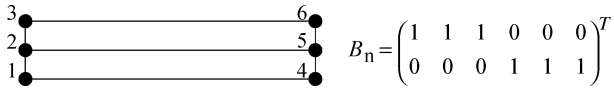

Fig. 4. Thin elements in nodal element analysis.

IV. Numerical Results

This section presents the numerical results, which demonstrate good performance by the IEC and EEC solvers in FE analyses involving thin elements. The following iterative solvers are used.

- Two IEC solvers [for (2a)]:
  — diagonal preconditioned CG (DPCG) solver;
  — incomplete Cholesky CG (ICCG) solver.
- An EEC preconditioned CG (PCG) solver [for (1)]. A symmetrized preconditioner based on the method described in Section II-B is used.

It should be noted that the DPCG method can be regarded as the Jacobi preconditioned CG method. From the viewpoint of the speed of convergence, the DPCG method invariably outperforms the Jacobi method.

When $B = O$, the IEC and EEC methods reduce to the conventional methods. In all tables, "O" indicates the results with respect to the conventional method, although the implementations are actually independent.

The 2-D and 3-D analyses are coded using M-code and Fortran, respectively. MATLAB R2008a and the Intel Fortran compiler 9.1 (/O2) are used. All computations are executed on a PC (Windows XP Professional x64, Core 2 Duo E6400, 2 GB RAM). The CG iterations are terminated when the relative residual norm with respect to (1) is less than 10^{-10}.

A. The 2-D Test Problem

Fig. 5 illustrates the 2-D test model and quadrilateral FE mesh with integer parameters $k = 16$ and $l = 4$. The Dirichlet boundary condition is imposed on the right and upper sides of the analyzed domain, and the Neumann boundary condition is imposed on the left and lower sides.

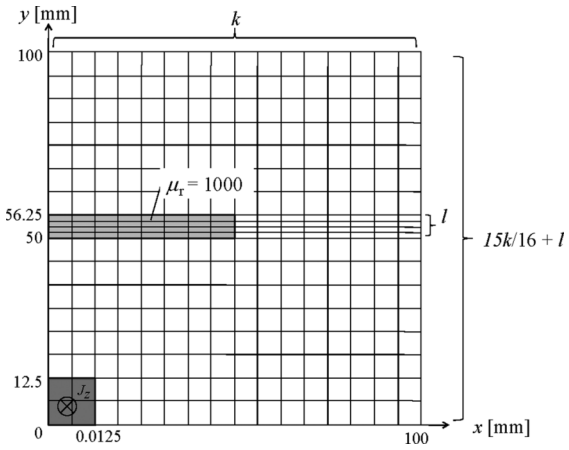

Fig. 5. The 2-D test problem and FE mesh ($k = 16$ and $l = 4$).

TABLE I
CONDITION NUMBER OF DIAGONAL PRECONDITIONED COEFFICIENT MATRIX FOR (2a) (2-D ANALYSIS)

Auxiliary Matrix B	Condition Number
O	1516
B_n	592.8

Quadrilateral FE mesh ($k = 16$ and $l = 16$) is used.

TABLE II
NUMBER OF CG ITERATIONS (2-D TEST ANALYSIS)

Auxiliary Matrix B	IEC		EEC
	DPCG	ICCG	PCG
O	660	147	195
B_n	365	89	111

Quadrilateral FE mesh ($k = 64$ and $l = 64$) is used.

1) Nodal Element Formulation: Finite nodal element formulation leads to the following coefficient matrix:

$$[A]_{ij} = \int_{\Omega} \nu \nabla N_i \cdot \nabla N_j dV \tag{9}$$

where the N_i are the nodal element basis functions.

2) Effect of IEC Formulations: Whereas (3) gives useful hints for the choice of B, the convergence of IEC solvers depends strongly on the condition number of the coefficient matrix of (2a). Here, the condition number is defined by the ratio of the maximum and minimum nonzero eigenvalues. Table I shows the condition number, which is given by eigenvalue analysis when $k = 16$ and $l = 16$. It can be confirmed that the IEC formulation using B_n decreases the condition number significantly.

3) Performance of the Iterative Solvers: Table II gives the convergence of the iterative solvers in 2-D analysis when $k = 64$ and $l = 64$. It shows the advantage of the IEC and EEC solvers in convergence characteristics.

The elapsed time depends strongly on the specific implementations when they are coded in M-code. However, the essential computation costs of the solvers per iteration are nearly proportional to the number of nonzero entries in the coefficient matrix, which is shown in Table III. Table III implies that the increase in the computation costs per iteration is moderate.

TABLE III
NUMBER OF DOFS AND NONZERO ENTRIES IN THE COEFFICIENT MATRIX (2-D TEST ANALYSIS)

Auxiliary Matrix B	Number of DOFs	Number of Nonzero Entries in the Coefficient Matrix
O	8,125	70,489
B_n	8,189	96,139

Quadrilateral FE mesh ($k = 64$ and $l = 64$) is used.

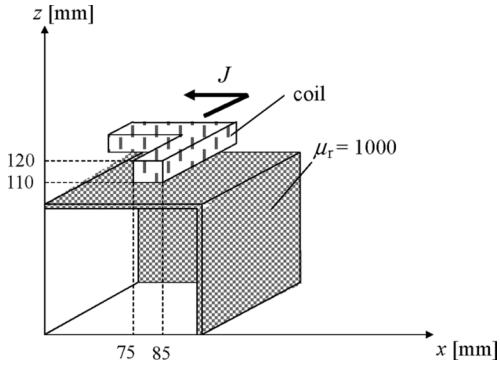

Fig. 6. The 3-D test model.

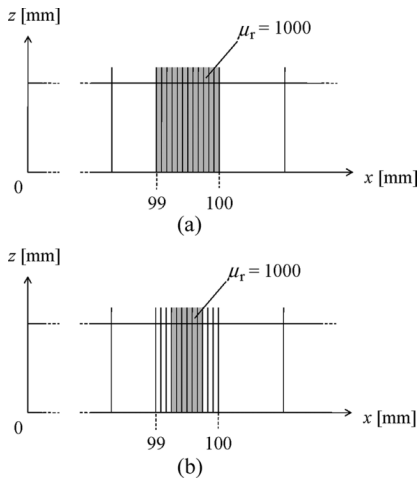

Fig. 7. FE mesh around the magnetic material. (a) Analysis 3-D1. (b) Analysis 3-D2.

B. The 3-D Test Problem

Fig. 6 shows the 3-D test model. The Neumann boundary condition is imposed on the xy-planes, while the Dirichlet boundary condition is imposed on the other boundaries. The analyzed domain is discretized by a hexahedral FE mesh.

Fig. 7 illustrates the FE mesh around the magnetic material. As shown in Fig. 7, two analyses are carried out with different thicknesses of the magnetic material, denoted by 3-D1 and 3-D2, respectively.

1) Edge-Element Formulation: Let the $\boldsymbol{N}_i$ be edge-element basis functions. Finite edge-element formulation derives the following coefficient matrix:

$$[A]_{ij} = \int_{\Omega} \nu(\nabla \times \boldsymbol{N}_i) \cdot (\nabla \times \boldsymbol{N}_j) dV. \tag{10}$$

2) Performance of the Iterative Solvers: Tables IV and V show the convergence of the iterative solvers in analyses 3-D1 and 3-D2, respectively. Whereas the IEC and EEC solvers using

TABLE IV
NUMBER OF CG ITERATIONS (ANALYSIS 3-D1)

Auxiliary Matrix B	IEC		EEC
	DPCG	ICCG	PCG
O	1280 (60)	571 (115)	348 (50)
B_e	271 (16)	134 (86)	79 (16)

Figures in parentheses denote the elapsed time (seconds)

TABLE V
NUMBER OF CG ITERATIONS (ANALYSIS 3-D2)

Auxiliary Matrix B	IEC		EEC
	DPCG	ICCG	PCG
O	1320 (60)	614 (119)	383 (52)
B_e	568 (32)	306 (119)	209 (40)
$B_e{}'$	274 (16)	131 (82)	79 (16)

Figures in parentheses denote the elapsed time (seconds)

TABLE VI
NUMBER OF DOFS AND NONZERO ENTRIES OF THE COEFFICIENT MATRIX (ANALYSIS 3-D1 AND 3-D2)

Auxiliary Matrix B	Number of DOFs	Number of Nonzero Entries of the Coefficient Matrix
O	438,204	14,033,916
B_e	447,524	17,827,356
$B_e{}'$	452,404	18,297,724

B_e drastically improve the convergence properties in analysis 3-D1, the effect deteriorates in analysis 3-D2. Table V demonstrates that the new auxiliary matrix B'_e is effective in accelerating the convergence in analysis 3-D2.

Figures in parentheses in Tables IV and V give the elapsed time. The DPCG (IEC) and PCG (EEC) solvers with suitable B outperform the other solvers with respect to the elapsed time. The PCG (EEC) solver has the additional advantage of not having to store the matrix AB in memory, which is different for the IEC solvers. The number of DOFs and nonzero entries in the coefficient matrix are given in Table VI.

V. CONCLUSION

In this paper, we present a formula, which provides helpful hints for determining the auxiliary matrix in the IEC and EEC methods. The formula reveals the reasonability of the method proposed in [3].

In addition, we suggest an enhanced strategy for determining the auxiliary matrix for thin elements. Numerical tests demonstrate the effect of the new strategy.

In our numerical tests, the EEC preconditioned CG solver based on the Gauss–Seidel method, which is regarded as an efficient implementation of an IEC solver, outperforms the other solvers, including the SDT.

APPENDIX I

When all diagonal entries are unity, the Jacobi iteration for the linear equations (2a) is expressed as follows:

$$\begin{pmatrix}\widetilde{\boldsymbol{y}}_1^{\text{new}}\\ \widetilde{\boldsymbol{y}}_2^{\text{new}}\end{pmatrix}=\begin{pmatrix}\widetilde{\boldsymbol{y}}_1\\ \widetilde{\boldsymbol{y}}_2\end{pmatrix}+\begin{pmatrix}\boldsymbol{b}-A(\widetilde{\boldsymbol{y}}_1+B\widetilde{\boldsymbol{y}}_2)\\ B^T\left[\boldsymbol{b}-A(\widetilde{\boldsymbol{y}}_1+B\widetilde{\boldsymbol{y}}_2)\right]\end{pmatrix}. \tag{A.1}$$

Here, $\widetilde{\boldsymbol{y}}_1$ and $\widetilde{\boldsymbol{y}}_2$ are the approximate solutions for $\boldsymbol{y}_1$ and $\boldsymbol{y}_2$, respectively. Replacing $\widetilde{\boldsymbol{y}}_1+B\widetilde{\boldsymbol{y}}_2$ by $\boldsymbol{z}$, we have

$$\boldsymbol{z}^{\text{new}}=\boldsymbol{z}+(I+BB^T)(\boldsymbol{b}-A\boldsymbol{z}) \tag{A.2}$$

that is

$$\boldsymbol{x}-\boldsymbol{z}^{\text{new}}=(I-A-BB^TA)(\boldsymbol{x}-\boldsymbol{z}). \tag{A.3}$$

From (A.3), the left inequality in (3) is immediately obtained.

Let $\boldsymbol{w}=\boldsymbol{u}+\boldsymbol{v}$, $\boldsymbol{u}\in R(B)$, and $\boldsymbol{v}\in S(B)$. Noting that $B^TA\boldsymbol{v}=0$ and $\|\boldsymbol{w}\|_A^2=\|\boldsymbol{u}\|_A^2+\|\boldsymbol{v}\|_A^2$, we have

$$\begin{aligned}\left\|(I-A-BB^TA)\right\|_A&=\sup\left\|(I-A-BB^TA)\boldsymbol{w}\right\|_A/\|\boldsymbol{w}\|_A\\&\le[(\alpha+\beta)\|\boldsymbol{u}\|_A+\gamma\|\boldsymbol{v}\|_A]\\&\quad\Big/\sqrt{\|\boldsymbol{u}\|_A^2+\|\boldsymbol{v}\|_A^2}\\&\le\sqrt{2}\max(\alpha+\beta,\gamma).\end{aligned} \tag{A.4}$$

In [4, eq. (3)], "$\sqrt{2}$" is incorrectly dropped.

APPENDIX II

Let L_1 and L_2 be the lower triangular parts of A and B^TAB, respectively. The Gauss–Seidel method for (2a) is expressed by

$$\begin{pmatrix}\widetilde{\boldsymbol{y}}_1^{\text{new}}\\ \widetilde{\boldsymbol{y}}_2^{\text{new}}\end{pmatrix}=\begin{pmatrix}\widetilde{\boldsymbol{y}}_1\\ \widetilde{\boldsymbol{y}}_2\end{pmatrix}+\begin{pmatrix}L_1&O\\ B^TA&L_2\end{pmatrix}^{-1}\times\begin{pmatrix}\boldsymbol{b}-A(\widetilde{\boldsymbol{y}}_1+B\widetilde{\boldsymbol{y}}_2)\\ B^T\left[\boldsymbol{b}-A(\widetilde{\boldsymbol{y}}_1+B\widetilde{\boldsymbol{y}}_2)\right]\end{pmatrix}. \tag{B.1}$$

The inverse matrix in (B.1) is given by

$$\begin{pmatrix}L_1&O\\ B^TA&L_2\end{pmatrix}^{-1}=\begin{pmatrix}L_1^{-1}&O\\ -L_2^{-1}B^TAL_1^{-1}&L_2^{-1}\end{pmatrix}. \tag{B.2}$$

After some calculation, we have

$$\begin{aligned}\boldsymbol{x}-\boldsymbol{z}^{\text{new}}&=\left(I-BL_2^{-1}B^TA\right)\left(I-L_1^{-1}A\right)(\boldsymbol{x}-\boldsymbol{z})\\&=G_2G_1(\boldsymbol{x}-\boldsymbol{z}).\end{aligned} \tag{B.3}$$

The matrix G_1 is identical to the iteration matrix of the Gauss–Seidel method for (1), and G_2 corresponds with the EEC procedure referred to in Section II-B.

REFERENCES

[1] T. Iwashita, T. Mifune, and M. Shimasaki, "Similarities between implicit multigrid method and A-phi formulation in electromagnetic field analysis," *IEEE Trans. Magn.*, vol. 44, no. 6, pp. 946–949, Jun. 2008.
[2] T. Mifune, S. Moriguchi, T. Iwashita, and M. Shimasaki, "A basic study on the implicit error correction method and explicit error correction method for the finite element method using a mesh with high aspect ratio," presented at the Tech. Meeting Static Apparatus Rotating Machinery of IEE Japan, (in Japanese) 2008, MAG-08-19/SA-08-7/RM-08-7, unpublished.
[3] A. Kameari, "Improvement of ICCG convergence for thin elements in magnetic field analysis using finite-element method," *IEEE Trans. Magn.*, vol. 44, no. 6, pp. 1178–1181, Jun. 2008.
[4] T. Mifune, T. Iwashita, and M. Shimasaki, "Convergence acceleration of iterative solvers for the finite element analysis using the implicit and explicit error correction methods," presented at the 13th Biennial IEEE Conf. Electromagn. Field Comput., 2008, PD1–11, unpublished.